

Phase transition kinetics of vanadium pentoxide

II. Theoretical results

L.D. Marks, V.A. Volpert and R. Ai

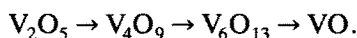
Center for Surface Radiation Damage Studies, Department of Material Science and Engineering, Northwestern University, Evanston, IL 60208, USA

Received 29 April 1992; accepted to publication 12 August 1992

Experimental data on the phase transformation kinetics in vanadium pentoxide due to surface oxygen loss are analyzed theoretically. A model for the process as a one-dimensional problem with oxygen loss from the surface and coupled interface and diffusion controlled growth modes is described. This model appears to match well the experimental data with reasonable numbers for the surface loss rate and diffusion constant. In particular, the model reproduces changes in the number of phase fronts as a function of electron beam flux. In addition, the analysis confirms that the effective diffusion constant is electron beam flux dependent.

1. Introduction

In a previous paper [1], experimental data on the phase transition kinetics in vanadium pentoxide as a function of beam flux were presented. We review, briefly, the main experimental results. For low values of the electron flux consecutive phase transformations occurred:



In this case three interfaces propagated into the sample. For higher values of the flux two phase transitions were observed:



In some cases two interfaces merged during the experiment, and the intermediate phase disappeared. For still higher values of the flux the original phase lost its stability, and phase separation in the bulk took place. As a result, a mixture of the two phases V_6O_{13} and VO appeared. The interface between $\text{V}_6\text{O}_{13} + \text{VO}$ and VO propagated into the sample.

In this paper we give a theoretical description of the process. To study the interface propagation we consider a free boundary problem (eqs. (2)–(5)

below). In accordance with the physics of the process the values u_{\pm} of the concentration on the interface cannot be considered as equilibrium ones, and we introduce equations for them (section 2). The condition on the interface has a natural form and generalizes the well-known limiting cases of diffusion control and interface control. The results of the numerical simulations and comparison of these results with the experimental data are presented in section 3.

2. Model

We begin with a brief, schematic description of the physical processes which take place during the experiment.

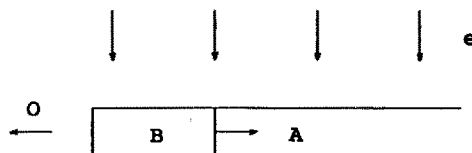


Fig. 1. Schematical representation of the process.

There is an electron flux which is perpendicular to the surface of a sample (fig. 1). It leads to a loss of oxygen from the material, probably oxygen ions due to a process such as interatomic Auger decay [2,3]. The loss of oxygen in effect creates oxygen vacancies at the surface which can diffuse into the material. At some level of oxygen deficiency a phase transformation to a lower oxide takes place at the side surface, and the interface appears near it. The interface propagates into the sample, and we have our original phase A to the right of it, and some new phase B to the left of the interface. This first phase transition can be followed by others.

Following this phase transition, the appropriate combination of oxygen vacancies/interstitials can diffuse in both original and transformed material. The actual diffusion process itself may be purely thermal, or may be electron assisted; for instance, the same interatomic Auger decay process which ejects oxygen at the surface can move oxygen around within the solid.

A complete model including oxygen vacancies, interstitials (and possible cation point defects), recombination and differing diffusion along both different crystallographic directions and in different phases would be exceedingly complicated. We have therefore chosen to make the following assumptions:

(a) We will consider all the oxygen atoms to be equivalent, and only consider that the oxygen diffuses by one mechanism.

(b) We will ignore the variations in the diffusion constants with crystallographic directions. In reality this may be the reason why different results have been obtained with the electron beam in different directions [4].

(c) We will assume that the diffusion constant does not vary between the different phases.

(d) We will assume that oxygen loss only occurs from the profile edge (side surface).

Experimentally, if new phases formed at the top and bottom surfaces this would have been readily visible. The exact reason why loss occurs primarily from the side surface is still unclear, but is probably due to the dipole polarization normal to the electron beam of energy loss with high energy electrons.

To describe the process we consider a simplified model of the process which includes diffusion of species in the bulk and the movement of the interface. The interface movement can be determined by the balance of mass and two additional relations connected with kinetics and thermodynamics of the phase transition. This gives a possibility to find the values of the concentration on the interface and the interface velocity.

There are two well-known limit cases of interface propagation: diffusion control and interface control (see, for example, refs. [5,6]). In the first case the interface position $y(t)$ as a function of time t changes slowly ($y(t) \sim \sqrt{Dt}$, where D is the diffusion coefficient), the values of the concentration on the interface u_+ and u_- are equal to the equilibrium values for the corresponding phases, and the interface velocity can be found from the balance of mass

$$D \left(\frac{\partial u}{\partial x} \Big|_{y-0} - \frac{\partial u}{\partial x} \Big|_{y+0} \right) + y'(u_+ - u_-) = 0. \quad (1)$$

Here

$$u_{\pm} = u(y(t) \pm 0, t),$$

$$\frac{\partial u}{\partial x} \Big|_{y \pm 0} = \frac{\partial u(y(t) \pm 0, t)}{\partial x},$$

$$y' = \frac{dy}{dt},$$

x is a spatial variable. The notations $y+0$ and $y-0$ mean that we take the limit values of the concentration and its gradient on the interface in the original and the new phases, respectively.

For the second case the propagation of the interface is fast, the equilibrium concentrations cannot be reached, and, moreover, there is no concentration step at the interface, $u_+ = u_-$. In this case the interface velocity can be expressed through the driving force of the interface. Under the assumption of small deviation from the equilibrium it has the form

$$y'(t) = k(u_e - u_+),$$

where u_e is the equilibrium value of the concentration, k is a constant.

For the coupled diffusion and interface controlled growth both of the balance of mass and

kinetics equations should be considered. Aziz and Kaplan [7] discuss a model for solidification of a two-component melt. Davi and Gurtin [8] consider the interface movement in a general formulation and suppose that the concentration step on the interface and the interfacial mass flux are some given functions of the chemical potential and its gradient.

In the case of the phase transition in metal oxides under irradiation, which we consider here, we should take into account the diffusion of oxygen in both the original and new phases, and consider a radiative boundary condition to describe the loss of oxygen through the side surface. For the process under consideration we cannot use the limiting cases of diffusion control and interface control. The physical idea of the process is that the concentration step on the interface is equal to zero at the moment that the interface appears, and then the step increases. This means that u_+ and u_- are not given constants, but some functions, and we should obtain additional equations for them. To do this we consider the balance of mass, taking into account the finite width of the interface, and the kinetics equation in the form which is close to that in ref. [7] and which gives a relation between the interface velocity and the driving force of the interface. The third condition on the interface determines the penetrability of the interface for the diffuse flux.

Thus we consider the free boundary problem

$$\frac{\partial u}{\partial t} = D \frac{\partial^2 u}{\partial x^2}, \quad 0 < x < y(t), \quad y(t) < x < L, \quad (2)$$

$$u|_{y \pm 0} = u_{\pm}, \quad (3)$$

$$x = 0: \quad \frac{\partial u}{\partial x} = hu, \quad x = L: \quad \frac{\partial u}{\partial x} = 0, \quad (4)$$

$$t = 0: \quad u = u_0. \quad (5)$$

Here u is the concentration of oxygen, $0 \leq x \leq L$, h a constant which characterizes the loss of oxygen through the side surface and which is supposed to be proportional to the value of the electron flux, and u_0 is the initial concentration of oxygen.

The balance of mass in the case of nonzero width of the interface has the form

$$l \frac{d}{dt} [su_+ + (1-s)u_-] = D \left(\frac{\partial u}{\partial x} \Big|_{y+0} - \frac{\partial u}{\partial x} \Big|_{y-0} \right) + y'(u_+ - u_-), \quad (6)$$

where l is a width of the interface, s is a constant, $0 < s < 1$, which characterizes the contribution of each phase in the balance of mass. In the case of constant u_+ and u_- or $l = 0$, eq. (6) coincides with (1). The balance of mass on the interface can also be written for u_+ and u_- separately:

$$sl \frac{du_+}{dt} = D \frac{\partial u}{\partial x} \Big|_{y+0} - Df + y'sl \frac{\partial u}{\partial x} \Big|_{y+0} + O(l^2),$$

$$(1-s)l \frac{du_-}{dt} = -D \frac{\partial u}{\partial x} \Big|_{y-0} + y'(u_+ - u_-) + Df - y'sl \frac{\partial u}{\partial x} \Big|_{y+0} + O(l^2).$$

Here f is a diffusive flux through the interface, $y' > 0$. Further in this paper we assume that $y'l \ll D$, which is in accordance with experimental data, and consider the case of impenetrable interface. In this case we have simplified the equations for u_+ and u_- :

$$sl \frac{du_+}{dt} = D \frac{\partial u}{\partial x} \Big|_{y+0}, \quad (7)$$

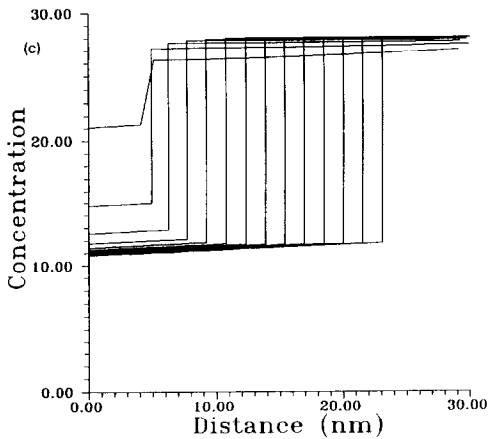
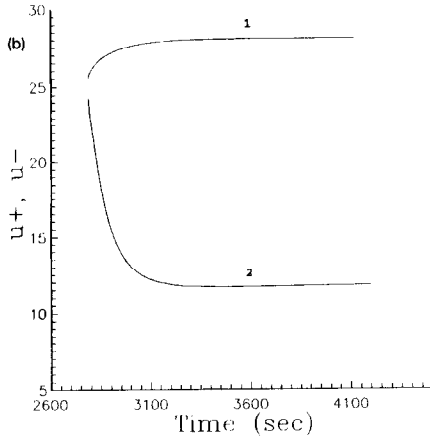
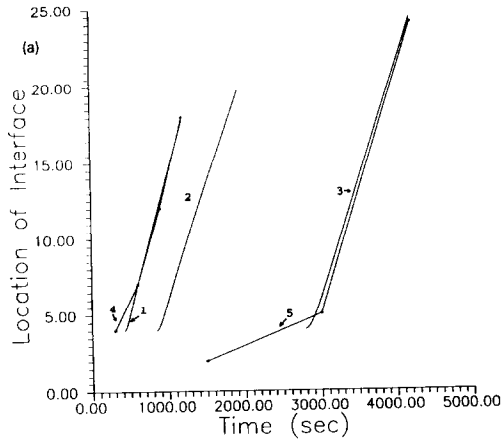
$$(1-s)l \frac{du_-}{dt} = -D \frac{\partial u}{\partial x} \Big|_{y-0} + y'(u_+ - u_-). \quad (8)$$

Similar to ref. [7] we express the interface velocity through the driving force of the interface:

$$y' = v_0 [1 - \exp(\Delta\mu/RT)].$$

Here v_0 is the maximum speed of the phase growth, $\Delta\mu$ the free energy difference responsible for the interface motion, R the gas constant, T the temperature which is supposed to be constant in these considerations. Assuming that the system is not far from the equilibrium we can consider the linearized form of the equation

$$y' = k[u_e - (su_+ + (1-s)u_-)], \quad (9)$$



where

$$k = v_0(\sigma_1 + \sigma_2),$$

$$u_e = (\sigma_1 u_e^+ + \sigma_2 u_e^-) / (\sigma_1 + \sigma_2),$$

u_e^+ and u_e^- are the equilibrium values of the concentration for the original and the new phases,

$$\sigma_1 = - \frac{\partial \sigma(u_e^+, u_e^-)}{\partial u_+}, \quad \sigma_2 = - \frac{\partial \sigma(u_e^+, u_e^-)}{\partial u_-},$$

$$s = \frac{\sigma_1}{\sigma_1 + \sigma_2}, \quad \sigma(u_+, u_-) = - \frac{\Delta \mu}{RT}.$$

We assume, finally, that the contribution of the phases in the free energy difference is the same as in the balance of mass. This means that the value of s in eqs. (7), (8) is equal to that in eq. (9).

To complete the formulation of the problem we should put a condition on the interface appearance. We denote by y_0 a critical nucleus size and suppose that the interface appears if

$$u |_{x=y_0} = u_{e_1}$$

for some $t = t_1$. We have

$$y(t_1) = y_0, \quad u_{\pm}(t_1) = u_{e_1}.$$

In the case of two interface propagation, the condition of the second interface appearance is similar:

$$u |_{x=z_0} = u_{e_2},$$

where $u_{e_2} < u_{e_1}$, and

$$z(t_2) = z_0, \quad v_{\pm}(t_2) = u_{e_2}.$$

Here u_{e_1} and u_{e_2} are thermodynamical mean values for the first and the second phase transitions, respectively, z_0 is a critical nucleus size for the third phase, v_+ and v_- the values of the concentration on the second interface, and $z(t)$ its location. We put also a condition on the

Fig. 2. (a) The location of the interface in time, (1-3) Numerical results: (1) $h = 0.011$, $D = 11.8$; (2) $h = 0.011$, $D = 5.9$; (3) $h = 0.004$, $D = 5.9$. (4, 5) Experimental results: (4) $F = 5.5$ A/cm²; (5) $F = 2.0$ A/cm². (b) The values of the concentration to the right (1) and to the left (2) of the interface. (c) Distribution of the concentration after the appearance of the interface.

intermediate phase disappearance. We suppose that it occurs if the size of this phase is less than a critical one, $z(t) - y(t) < y_0$.

The model we consider here does not describe the phase separation which was observed experimentally for the high fluxes, which requires a more complicated model. In this paper we consider only the phase transition due to the movement of the interface $y(t)$. Moreover, we consider the case when the interface is planar. In reality, it is not the case for the high fluxes when the transition from $V_6O_{13} + VO$ into VO occurs. Nevertheless, since the particles are sufficiently small and the interface is close to a plane one [1], we can expect that a one-dimensional model describes the process.

3. Numerical solution and comparison with experimental results

A finite-difference method using the Thomas algorithm (see, for example, ref. [9]) was used for the numerical computations of eqs. (2)–(5), (7)–(9). We used an implicit scheme, and iterated to calculate the location of the interface and the distribution of the concentration. The accuracy of the computations was verified by decreasing the space and time steps.

We considered the values of parameters which correspond, approximately, to the phase transformation in vanadium oxides: $u_0 = 50 \text{ nm}^{-3}$, $u_e = 25 \text{ nm}^{-3}$, $y_0 = 4 \text{ nm}$, $l = 2 \text{ nm}$, $s = 0.5$. The procedure was to vary the values of k , h , and D so as to obtain the best approximation to the experimental results. First of all we chose h and D to obtain the time of the interface appearance which corresponds to the experimental data. Then we take the value of k to obtain the appropriate value of the interface velocity.

Fig. 2a (curves 3 and 5) shows the location of the interface versus time obtained numerically and experimentally (for the value of the electron flux $F = 2.0 \text{ A/cm}^2$). Here $k = 0.0015 \text{ nm}^4/\text{s}$, $h = 0.004 \text{ nm}^{-1}$, $D = 5.9 \text{ nm}^2/\text{s}$. A significant point is that these numbers are quite reasonable, which provides some confidence in the model. We note that the initial oxygen loss rate (Dhu_0)

of about one atom/ $\text{nm}^2 \cdot \text{s}$ is also reasonable. As usual, an approximation of experimental data can be obtained not only for these values of parameters but for some range of values. For example, we can change the value of h in a few times, but we cannot change the order of the value. Considerable increase of h and corresponding decrease of D changes the behavior of solution; the interface velocity does not tend to a constant in the given time interval, but decreases rather quickly. Contrary, decreasing of h implies increasing of D . The dependence of D on h is rather strong, and the diffusion coefficient becomes unreasonably large for small values of h .

We note that the experimental curve has a more prolonged induction period (for which the interface velocity increases) than the numerical one. This can be caused by a particular penetrability of the interface for the diffusive flux and by the dependence of the penetrability on time.

When the induction period is over, the interface velocity becomes close to a constant. Such behavior of the interface velocity corresponds to the dependence of u_+ and u_- on time (fig. 2b). At the moment $t = t_0$ when the interface appears $u_+ = u_- = u_e$, and the interface velocity is equal to zero. Then u_+ increases, u_- decreases, and they tend to some constant value, as does $y'(t)$.

The distribution of the concentration versus time after the appearance of the interface is shown in fig. 2c. We note that the distribution of the concentration to the right of the interface is close to a constant one, and the concentration profile to the left of the interface close to linear.

The values of the parameters which give an approximation to the experimental results depend on the electron flux. We suppose that h is related to the value of the flux. The experimental curves 4 and 5 on fig. 2a correspond to the values of flux $F_1 = 5.5 \text{ A/cm}^2$ and $F_2 = 2.0 \text{ A/cm}^2$, respectively. It was pointed out above that the approximation of curve 5 was obtained for $h_2 = 0.004 \text{ nm}^{-1}$, $D_2 = 5.9 \text{ nm}^2/\text{s}$. Thus, to obtain the approximation of curve 4 we should take $h_1 = 0.011 \text{ nm}^{-1}$ (fig. 2a, curve 2). We see that this does not describe the experimental data. Changing k cannot give a better approximation since the time of the interface appearance does not

depend on it. So the only way to improve the approximation in the frameworks of our model is to increase the diffusion coefficient. Curve 1 in fig. 2a is obtained for $h_1 = 0.011 \text{ nm}^{-1}$ and $D_1 = 11.8 \text{ nm}^2/\text{s}$. Thus we can conclude that the diffusion coefficient depends on the electron flux. Depending on temperature, the diffusion coefficient may not depend on the value of flux, depend on it linearly, or depend on it as a square root [10]. In our case $\sqrt{F_1/F_2} \approx 1.7$, $D_1/D_2 = 2.0$. This means, probably, that the last case takes place, and the diffusion is determined by irradiation produced defects.

We consider now the results of numerical analysis of the problem (2)–(5), (7)–(9) for the case when two interfaces propagate into the sample one after another. Fig. 3 shows the location of the interfaces for the following values of the parameters: $D = 5.9 \text{ nm}^2/\text{s}$, $h = 0.0036 \text{ nm}^{-1}$, $u_{e1} = 25 \text{ nm}^{-3}$, $y_0 = z_0 = 1 \text{ nm}$. We note that the value of h corresponds to the value of the electron flux $F = 1.8 \text{ A/cm}^2$ for which the propagation of two interfaces was observed experimentally. The values y_0 and z_0 are not very important for a description of the qualitative behavior of solutions, and we chose them to illustrate this behavior more clearly.

We see that the first interface appears and propagates into the sample. We know that the value of the concentration to the left of the

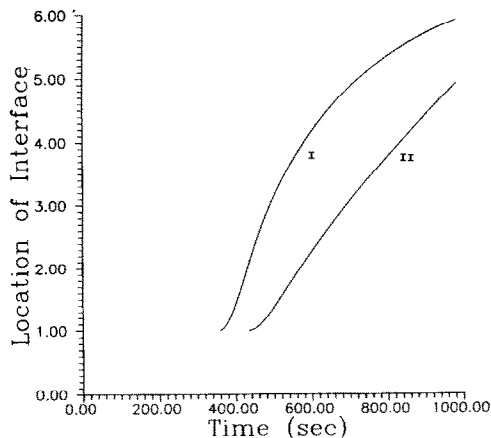


Fig. 3. Two interface propagation: the location of the interface in time. (I) First interface, (II) second interface.

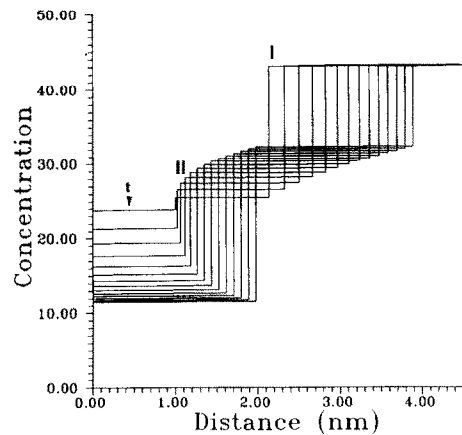


Fig. 4. Two interface propagation: distribution of the concentration.

interface decreases rather quickly (see fig. 2b). The condition for the second interface to appear is satisfied in this case for a smaller value of time, so the first phase transformation accelerates the beginning of the second one. When the second interface appears, the distance between them is more than y_0 . In the beginning the velocity of the first interface is greater than the velocity of the second one, but then it decreases as well as the distance between the interfaces. The calculations are finished when this distance is equal to y_0 , and the second phase disappears.

The distribution of the concentration is close to a linear one on the interval $0 \leq x \leq z(t)$, and it is close to a constant for $x \geq y(t)$. The function $u(x, t)$ does not depend on x practically in the interval $z(t) < x < y(t)$, but increases as a function of time (fig. 4). It leads to a decrease of the first interface velocity, and we can say that the second interface slows down the first interface. For the second interface, increasing the concentration to the right is compensated by decreasing the concentration to the left due to diffusion and mass loss on the boundary, and the second interface velocity decreases slowly.

If we increase h from the value of 0.0036 to the value of 0.004 nm^{-1} then only one interface appears. Numerical simulations show that in this case the first interface appears, and it propagates into the sample similar to the variant with the

lower value of h . But the condition of the second interface appearance is satisfied rather quickly due to the increasing of h , and the distance between the interfaces is small. This leads to the disappearance of the second phase, and we have only one phase transformation. The value of u_{e_2} is chosen to obtain qualitative agreement with experimental results: the transition of two interface propagation to one interface propagation under increasing electron flux.

We emphasize that the numerical simulations show the same results as the experimental data: the second interface slows down to the first one, they merge, and the intermediate phase disappears. This confirms that the process is not pure diffusion controlled. Indeed, if this was the case the interfaces cannot merge: when the second interface comes nearer to the first one, the concentration gradient between them increases, and it accelerates the first interface while decelerating the second.

4. Discussion

We will discuss first the numerical results herein, and then give a more general discussion of both this and companion paper [1].

4.1. Numerical analysis

Obviously we have only used a simplified model herein, and as stated earlier there are approximations. However, it would appear that this model reproduces, without major ad-hoc assumptions, both the character of the experimental data at one flux and the changes in the phase transition routes as a function of flux. The experimental results show the presence of three interfaces for low values of flux. We believe that the model should be extendable to this case also.

It is appropriate here to make some comments about the conventional usage of "diffusion" and "interface" controlled growth modes. Considering eqs. (7)–(9) there are two limiting cases:

(a) For a small concentration step the rate limiting term is the kinetic constant k .

(b) With a large concentration step the rate limiting term is the diffusion constant.

These two cases correspond to the limits of interface and diffusion controlled growth, respectively. If the interface velocity tends to some positive constant then the process is considered to be interface controlled. However the results presented above show that a constant velocity of the interface does not necessarily imply the absence of a concentration step, which is required for interface control. The regimes observed have the features of both interface and diffusion controlled processes.

4.2. General

With the confidence provided by the success of these numerical simulations, it appears now to be possible to present a general model of DIET (desorption induced by electronic transition) in oxides at least as far as the issue of materials changes. Much of the information is available in more tentative form in earlier papers [11,12].

The pump for the process is loss of oxygen from the surface. There are many models for this process which have been proposed [13,14], which one(s) are appropriate as yet being unclear.

Oxygen loss at the surface leads to point defects which diffuse into material. Based upon the analysis herein the effective diffusion constant is electron beam flux dependent. We believe that the same Knotek–Feibelman interatomic Auger process occurring in the bulk is enhancing the diffusion constant. Point defect migration dominates, and diffusive (not displacive) phase transitions taken place to higher symmetry, lower oxides; lower oxides which do not have the appropriate symmetry do not arise [15]. The kinetics of these phase transformations depends upon the pumping rate and the (electron enhanced) diffusion constant. Experimental variations in the kinetics both with orientation (anisotropies in both the diffusion constant and the interface mobility) and the electron flux change the phase transition routes.

Although a wide range of experimental phenomena have been observed [16–20], all of it appears to fit within the well accepted materials behavior models.

Acknowledgement

This work was supported by the Air Force Office of Scientific Research on grant number AFOSR-90-0045.

References

- [1] R. Ai, H.J. Fan and L.D. Marks, *Surf. Sci.* 280 (1993) 369.
- [2] M.L. Knotek and P.J. Feibelman, *Phys. Rev. Lett.* 40 (1978) 964.
- [3] M.L. Knotek and P.J. Feibelman, *Phys. Rev. B* 18 (1978) 6531.
- [4] J. Strane, MS Thesis, Northwestern University, 1988.
- [5] J.W. Christian, *The Theory of Transformations in Metals and Alloys*, 2nd ed. (Pergamon, New York, 1981).
- [6] M. Hillert, *Metall. Trans.* 6 A (1975) 5.
- [7] M.J. Aziz and T. Kaplan, *Acta metall.* 36 (1988) 2335.
- [8] F. Davi and M.E. Gurtin, *J. Appl. Math. Phys.* 41 (1990) 782.
- [9] T. Shih, *Numerical Heat Transfer* (Hemisphere, New York, 1984).
- [10] K.C. Russel, *Prog. Mater. Sci.* 28 (1984) 229.
- [11] S.R. Singh and L.D. Marks, *Philos. Mag. Lett.* 60 (1989) 31.
- [12] R. Ai, H.J. Fan, P.C. Stair and L.D. Marks, *Mater. Res. Soc. Symp. Proc.* 157 (1990) 599.
- [13] *Desorption Induced by Electronic Transitions, DIET I*, Eds. N.H. Tolk, M.M. Traum, J.C. Tully and T.E. Madey, Vol. 24 of *Springer Series in Chemical Physics* (Springer, New York, 1983).
- [14] *Desorption Induced by Electronic Transitions, DIET II*, Eds. W. Brenig and D. Menzel, Vol. 4 of *Springer Series in Surface Sciences* (Springer, New York, 1985).
- [15] J.P. Zhang and L.D. Marks, *Surf. Sci.* 222 (1989) 13.
- [16] L.D. Marks, A.K. Petford and M. O'Keefe, *Surf. Sci.* 172 (1986) 496.
- [17] M.R. McCartney and D.J. Smith, *Surf. Sci.* 221 (1989) 214.
- [18] M.I. Buckett and L.D. Marks, *Surf. Sci.* 232 (1990) 353.
- [19] H. Fan and L.D. Marks, *Ultramicroscopy* 31 (1989) 357.
- [20] J. Strane, L.D. Marks, D.E. Luzzi, M.I. Buckett, J.P. Zhang and B.W. Wessels, *Ultramicroscopy* 25 (1988) 253.